Exchange Interaction Mediated by O−H···O Hydrogen Bonds: Synthesis, Structure, and EPR Study of the Paramagnetic Organometallic Carboxylic Acid (η^7-C_7H_7)V(η^5-C_5H_4COOH)§

Ch. Elschenbroich,* O. Schiemann, O. Burghaus, and K. Harms

Contribution from the Fachbereich Chemie, Philipps-Universität, D-35032 Marburg, Germany

Received December 27, 1996⊗

Abstract: Lithiation of trovacene [(η^7-**tro**pylium)**va**nadium(η^5-**c**yclop**en**tadi**e**nyl)] (**1**•) and appropriate subsequent reactions afforded trovacenyl carboxylic acid (η^7-C_7H_7)V(η^5-C_5H_4COOH) (**2**•) and its anhydride [(η^7-C_7H_7)V(η^5-C_5H_4CO)]$_2$O (**3**••). The deuterated acid **2**•-d_1 was also prepared; **2**•, **2**•-d_1, and **3**•• were characterized by X-ray structural analysis. The dimeric hydrogen bonded structure of **2**• which is found in the crystal also prevails in aprotic, nonpolar solvents and gives rise to a biradical EPR spectrum from which the electron exchange coupling constant $J = -0.011$ cm^{-1} can be determined via computer simulation. Thus, exchange interaction across eight bonds is observable even though the spacer contains weak hydrogen bonds. Considerably stronger exchange coupling ($J = -0.345$ cm^{-1}) is displayed by the anhydride **3**••. The EPR spectrum of **2**• in toluene is temperature dependent as expected for the equilibrium 2 (**2**•) ⇌ (**2**•)$_2$ which leads to the superposition of monomer and dimer spectra at ratios governed by temperature. The enthalpy of dimerization can thus be derived; it amounts to −11.8 kcal mol^{-1} for **2**• and −15.2 kcal mol^{-1} for **2**•-d_1. The ^{1}H NMR spectrum of the radical **2**• reveals the positive contact shift $\Delta\delta = 3$ ppm for the carboxylic proton, relative to the chemical shift observed for the diamagnetic organometallic acid Cr(η^6-C_6H_5COOH)$_2$. Conceivably, the finite spin density on the carboxyl group, present in the monomer **2**•, contributes to the exchange interaction displayed by the hydrogen bonded dimer (**2**•)$_2$. The redox potential $E_{1/2}$ (**2**$^{+/0}$) and the hyperfine coupling constant a(^{51}V, **2**•) are pH dependent. In the former case, a Nernst−Clark plot furnishes the pK_s values of 4.4 for neutral **2**• and 1.85 for the cation **2**$^+$. A similar value, pK_s(**2**•) = 3.7, is read off the plot a(^{51}V, **2**•) versus pH.

Introduction

Details of the mechanisms of intramolecular electron transfer propagated by bridging units[1]—in particular those concerning the primary step in photosynthesis[2]—are still controversial; one aspect is dealing with the question whether single-step superexchange or a two-step path with a discrete intermediate prevails. Whereas the study of intramolecular electron transfer requires highly sophisticated techniques of time resolved spectroscopy, another phenomenon of intramolecular communication, namely spin exchange interaction in biradicals, can be explored in a more straightforward fashion by measuring the exchange coupling constant J via EPR. In fact, it has been suggested repeatedly in the literature that electron transfer and spin exchange may have several determining factors in common.[3]

A structural unit which is part of ET pathways in noncovalently linked proteins as well as in photosynthetic model systems is the hydrogen bond.[4] Since there has been an upsurge in interest in hydrogen bonded organometallic species,[5] we combined the two seemingly unrelated fields and prepared the paramagnetic organometallic acid (η^7-C_7H_7)V(η^5-C_5H_4COOH), trovacenylcarboxylic acid **2**•, in order to study electron−electron spin−spin exchange in the dimer (**2**•)$_2$. For the purpose of comparison, the deuterated acid **2**•-d_1 and the binuclear anhydride **3**•• were also synthesized.

Experimental Section

All manipulations were carried with exclusion of air under dinitrogen or argon (CV). Physical measurements were performed with the equipment specified previously.[6] Cyclovoltammetric (CV) traces for **2**• and **3**• were recorded in the medium dimethoxyethane/*n*-Bu_4NClO_4 at −35 °C employing a glassy carbon working electrode, a platinum wire counter electrode, and a SCE reference electrode; the scan rate was 0.1 V s^{-1}. The study of the pH dependence of the redox potential

§ Trovacene Chemistry. Part 1.

⊗ Abstract published in *Advance ACS Abstracts,* July 15, 1997.

(1) (a) Fox, M. A. *Chem. Rev.* **1992**, *92*, 365 for leading references. See also articles in this issue. (b) Marcus, R. A.; Sutin, N. *Biochim. Biophys. Acta* **1985**, *811*, 265. (c) Onuchic, J. N.; Beratan, D. N. *J. Chem. Phys.* **1990**, *92*, 722. (d) Paulson, B. P.; Curtiss, L. A.; Bal, B.; Closs, G. L.; Miller, J. R. *J. Am. Chem. Soc.* **1996**, *118*, 378.

(2) (a) Kurreck, H.; Huber, M. *Angew. Chem., Int. Ed. Engl.* **1995**, *34*, 849, for leading references. (b) Moser, Ch. C.; Keske; J. M.; Warncke, K.; Farid, R. S.; Dutton, P. L. *Nature* **1992**, *355*, 796. (c) Pelletier, H.; Kraut, J. *Science* **1992**, *258*, 1748. (d) Beratan, P. N.; Onuchic, J. N.; Winkler, J. R.; Gray, H. B. *Science* **1992**, *258*, 1740. (e) Hunter, C. A.; Hyde, R. K. *Angew. Chem., Int. Ed. Engl.* **1996**, *35*, 1936.

(3) (a) Ramasami, R.; Endicott, J. F. *J. Am. Chem. Soc.* **1985**, *107*, 389. (b) Bertrand, P. *Chem. Phys. Lett.* **1985**, *113*, 104. (c) Blondin, G.; Girerd, J.-J. *Chem. Rev.* **1990**, *90*, 1359. (d) Forbes, M. D. E.; Ball, J. D.; Avdievich, N. I. *J. Am. Chem. Soc.* **1996**, *118*, 4707. (e) Coffmann, R. E.; Buettner, G. R. *J. Phys. Chem.* **1979**, *83*, 2387.

(4) (a) Sessler, J. L.; Wang, B.; Harriman, E. *J. Am. Chem. Soc.* **1993**, *115*, 10418 and references given therein. (b) Roberts, J. A.; Kirby, J. B.; Nocera, D. G. *J. Am. Chem. Soc.* **1995**, *117*, 8051. (c) Harriman, A.; Kubo, Y.; Sessler, J. L. *J. Am. Chem. Soc.* **1992**, *114*, 388. (d) Berman, A.; Izraeli, E. S.; Levanon, H.; Wang. B.; Sessler, J. L. *J. Am. Chem. Soc.* **1995**, *117*, 8252. (e) Hayashi, T.; Miyahara, T.; Kumazaki, S.; Ogoshi, H.; Yoshihara, K. *Angew. Chem., Int. Ed. Engl.* **1996**, *35*, 1964. (f) Cukier, R. I. *J. Phys. Chem.* **1994**, *98*, 2377. (g) Zhao, X. G.; Cukier, R. I. *J. Phys. Chem.* **1995**, *99*, 945. (h) Miyasaka, H.; Tabata, A.; Kamada, K.; Mataga, N. *J. Am. Chem. Soc.* **1993**, *115*, 7335. (i) Turró, C.; Chang, C. K.; Leroi, G. E.; Cukier, R. I.; Nocera, D. G. *J. Am. Chem. Soc.* **1992**, *114*, 4013.

(5) (a) Braga, D.; Grepioni, F.; Tedesco, E.; Biradha, K.; Desiraju, G. R. *Organometallics* **1996**, *15*, 2692 and previous papers in the series. (b) Beer, P. D.; Drew, M. G. B.; Graydon, A. R.; Smith, D. K.; Stokes, S. E. *J. Chem. Soc., Dalton Trans.* **1995**, *403*. (c) Shubina, S.; Belkova, N. V.; Krylov, A. N.; Vorontsov, E. V.; Epstein, L. M.; Gusev, D. G.; Niedermann, M.; Berke, H. *J. Am. Chem. Soc.* **1996**, *118*, 1105. (d) Davies, G. J.; Veldmann, N.; Grove, D. M.; Spek, A. L.; Lutz, B. T. G.; van Koten, G. *Angew. Chem., Int. Ed. Engl.* **1996**, *35*, 1550. (e) Iwai, K.; Katada, M.; Motoyama, I.; Sano, H. *Bull Chem. Soc. Jpn.* **1987**, *60*, 1961.

(6) Elschenbroich, Ch.; Metz, B.; Neumüller, B.; Reijerse, E. *Organometallics* **1994**, *13*, 5072.

S0002-7863(96)04445-9 CCC: $14.00

$\mathbf{2}^{+/0}$ and of the hyperfine coupling constant $a(^{51}V, \mathbf{2}^{\bullet})$ was performed in buffered aqueous solution ($NaH_2PO_4/CH_3COONa/H_3BO_3$, 0.2 M each) at 25 °C and adjustment of the required pH value with HCl or NaOH.

The simulation of the EPR spectra was carried out with the least squares fit program CWSIM[7a] on a Power Mac 7100/80 AV. A downhill simplex fitting method was used, expressions for binuclear exchange coupled systems were taken from ref 7b. An extension to second order was provided by P. H. Rieger[7c] and incorporated into CWSIM. Inclusion of the m_I-dependence of the line widths[7d] considerably improved the fit between experimental and simulated spectra. It should be stated, however, that, as opposed to the parameters $a_{iso}(^{51}V)$ and g_{iso}, for increasing J, the exchange coupled spectra become increasingly insensitive to changes of the latter parameter. Accordingly, an uncertainty in the value of J can arise, which may reach the order of 1000 G in the case of $J/a(^{51}V) = 30$.

(η^7-C_7H_7)V(η^5-C_5H_4COOH) ($\mathbf{2}^{\bullet}$). To a solution of 0.5 g (2.4 mmol) of (η^7-C_7H_7)V(η^5-C_5H_5) ($\mathbf{1}^{\bullet}$) in 100 mL of diethyl ether is added *n*-butyllithium (2.4 mmol, 1.5 mL of a 1.6 M solution in hexane). After being stirred at room temperature for 12 h CO_2 gas is introduced for 30 min, the diethyl ether is removed *in vacuo*, and the residue is dissolved in H_2O. The aqueous solution is acidified with anaerobic HCl (1%) to pH ≈ 5, the green precipitate of $\mathbf{2}^{\bullet}$ is collected and dried in high vacuum. Yield: 0.25 g, 42%. Single crystals suitable for X-ray diffraction are produced from the acid chloride $\mathbf{4}^{\bullet}$ (vide infra) via hydrolysis: 100 mg of $\mathbf{4}^{\bullet}$ are dissolved in 2 mL of tetrahydrofuran and 5 mL of water, and the unstirred solution is kept at 0 °C for 2 days. ^{1}H NMR (500 MHz, THF-d_8, 23 °C): δ 14.1 (b, 1H, COOH); δ 127.6 (b, 2H, H3 and H4, Cp); δ 146.2 (b, 2H, H2 and H5, Cp); δ 315.0 (b, 7H, tropylium). IR (KBr): ν_{CH} 3000 cm^{-1}, ν_{OH} 2650 cm^{-1}, $\nu_{C=O}$ 1672 cm^{-1}, ν_{C-O} 1308 cm^{-1}. MS (EI), *m/e* (rel intensity): 251 (M^+, 68); 159 (100); 129 (25); 91 (10); 67 (20); 42 (23). MS (FD, toluene) *m/e*: 251 (M^+). Anal. Calcd for $C_{13}H_{12}O_2V$: C, 62.16; H, 4.82. Found: C, 61.95; H, 4.86.

(η^7-C_7H_7)V(η^5-C_5H_4COOD) ($\mathbf{2}^{\bullet}$-d_1). Single crystals of the deuterated acid ($\mathbf{2}^{\bullet}$-d_1) were obtained from ($\mathbf{4}^{\bullet}$) and D_2O/THF as described above for ($\mathbf{2}^{\bullet}$). ^{1}H-NMR (500 MHz, THF-d_8, 23 °C): O−H absent, δ 127.6 (b, 2H, H3 and H4, Cp); δ 146.2 (b, 2H, H2 and H5, Cp); δ 315.0 (b, 7H, tropylium). IR (KBr): ν_{OH} absent; ν_{OD} 2100 cm^{-1}, $\nu_{C=O}$ 1673 cm^{-1}, ν_{C-O} 1305 cm^{-1} MS (EI), *m/e* (rel intensity): 252 (M^+ $\mathbf{2}^{\bullet}$-d_1, 88); 251 (M^+ $\mathbf{2}^{\bullet}$, 18).

[(η^7-C_7H_7)V(η^5-C_5H_4CO)]$_2$O ($\mathbf{3}^{\bullet\bullet}$). To a suspension of 0.25 g (1 mmol) of $\mathbf{2}^{\bullet}$ in 5 mL of toluene is added under vigorous stirring at 0 °C during 15 min *n*-butyllithium (1 mmol, 0.6 mL of a 1.6 M solution in hexane). The brown precipitate of (η^7-C_7H_7(V(η^5-C_5H_4COOLi) is filtered off and suspended in 3 mL of toluene. At 0 °C under stirring oxalyl chloride (0.04 mL, 0.45 mmol) is added. The solvent is stripped off *in vacuo* and the residue is dissolved in 5 mL of THF. Column chromatography at silylated silica gel yields a first band of the acid chloride $\mathbf{4}^{\bullet}$ (elution with petroleum ether) and a second band containing the acid anhydride $\mathbf{3}^{\bullet\bullet}$ (elution with toluene); yield: 0.15 g, 32%. Single crystals suitable for X-ray diffraction were grown from CH_2Cl_2/petroleum ether. IR (toluene): ν_{CH} 3000 cm^{-1} $\nu_{C=O}$ 1774 cm^{-1}, $\nu_{C=O}$ 1716 cm^{-1}, ν_{C-O} 1097 cm^{-1}. MS (EI), *m/e* (rel intensity): 484 (M^+, 31); 234 (100), 206 (45), 128 (32). Anal. Calcd for $C_{26}H_{22}O_3V_2$: C, 64.46; H, 4.55. Found: C, 64.35; H, 5.74.

(η^7-C_7H_7)V(η^5-C_5H_4COCl) ($\mathbf{4}^{\bullet}$). The directions follow those given for $\mathbf{3}^{\bullet\bullet}$ with the modification that 0.9 mmol of oxalyl chloride are added at room temperature. The first band, which is eluted with toluene, contains $\mathbf{4}^{\bullet}$ as the principal reaction product. Removal of solvent yields 0.12 g (44%) of $\mathbf{4}^{\bullet}$ as a green material. MS (EI), *m/e* (rel intensity): 269 (M^+, 16); 177 (100); 91 (91). EPR (toluene): $g_{iso} = 1.9829$, $g_{\parallel} = 1.9948$, $g_{\perp} = 1.9769$; $a_{iso}(^{51}V) = -7.35$ mT, $A_{\parallel}(^{51}V) = -1.85$ mT, $A_{\perp}(^{51}V) = -10.10$ mT. CV (DME/TBAP, 2mm GC/SCE/Pt, $\upsilon = 0.1$ V s^{-1}, −35 °C): $E_{1/2}(+/0)$ 0.64 V, $\Delta E_{1/2}$ 84 mV, $I_{pa/pc}$ 0.93; $E_{pa}(+2/+1)$ 1.237 V; $E_{pc}(0/-1)$ −2.190. Anal. Calcd for $C_{13}H_{11}ClOV$: C, 57.91; H, 4.11. Found: C, 58.39; H, 4.80.

(7) (a) Burghaus, O. Unpublished. (b) Mabbs, F. E. *Chem. Soc. Rev.* **1993**, 313. (c) Rieger, P. H. Personal communication. (d) Bertini, I.; Martini, G.; Luchinat C. *Handbook of Electron Spin Resonance*; Poole, Jr., C. P., Farach, H. A., Eds.; AIP Press: New York, 1995.

Scheme 1

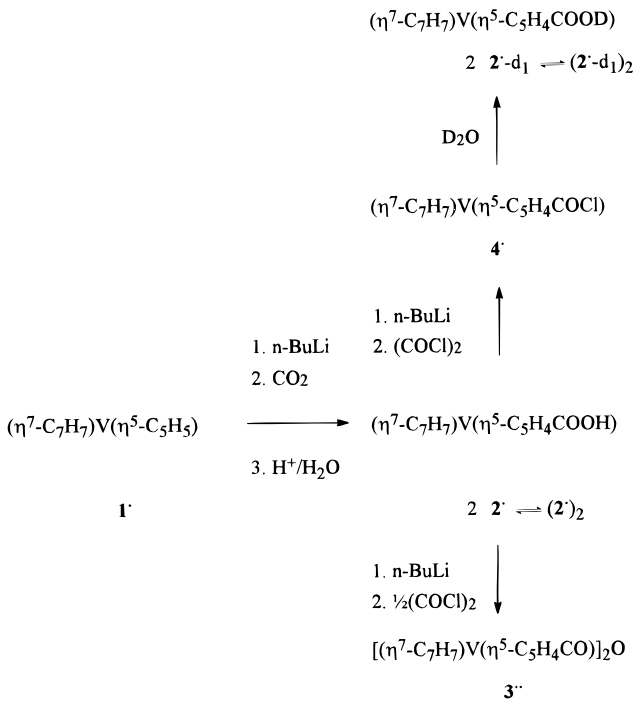

Crystallography. The crystal and refinement data for compounds $\mathbf{2}^{\bullet}$, $\mathbf{2}^{\bullet}$-d_1, and $\mathbf{3}^{\bullet\bullet}$ are given in Table 1. All non-hydrogen atoms were refined anisotropically; hydrogen atoms were refined isotropically.

Results and Discussion

The reactions leading to the new derivatives of (η^7-**tro**pylium)**va**nadium(η^5-**c**yclop**en**tadi**e**nyl) (trovacene, $\mathbf{1}^{\bullet}$) are given in Scheme 1. Single crystals of $\mathbf{2}^{\bullet}$, $\mathbf{2}^{\bullet}$-d_1, and $\mathbf{3}^{\bullet\bullet}$ were subjected to **X-ray diffraction** (Table 1), structural plots are displayed in Figures 1 and 2. Whereas in the acid dimer $(\mathbf{2}^{\bullet})_2$ the two sandwich axes are parallel, (intermetal distance V···V = 10.10 Å) an orthogonal disposition is encountered for the anhydride $\mathbf{3}^{\bullet\bullet}$ (V···V = 6.66 Å). This is immaterial for the discussion of electron exchange coupling in fluid solution, however, since in both cases conformational flexibility must be assumed. For the same reason, the shorter interdimer distances V···V (6.21, 6.33, 6.80, 7.00 Å), which exist in the solid state of $\mathbf{2}^{\bullet}$, do not constitute a problem since in liquid solution; only the intervanadium distance of the dimer $\mathbf{2}^{\bullet}$ enters into the discussion. The structural parameters of the trovacenyl units (Tables 2 and 3) are virtually identical in $\mathbf{2}^{\bullet}$ and $\mathbf{3}^{\bullet\bullet}$ since the metal ring−centroid distances of 146 and 191 pm, respectively, are governed by the constancy of the metal−carbon bond lengths.[8] The hydrogen bond motif is that of an eight-membered ring [graph set $R_2^2(8)$[9a]]; the distances O−H, H···O and O−H···O are very similar to those of butylbenzoic acid[9b] and its $Cr(CO)_3$ adduct.[9c] Within the limits set by the standard deviations, the structural features of the hydrogen bridges in $\mathbf{2}^{\bullet}$ and in its deuterated analog $\mathbf{2}^{\bullet}$-d_1 are identical.

By means of **cyclic voltammetry**, reversible couples $V^{+1/0}$ are observed for $\mathbf{2}^{\bullet}$ ($E_{1/2} = 0.48$ V, $\Delta E_{1/2} = 74$ mV, $i_a/i_c = 0.92$) and $\mathbf{3}^{\bullet\bullet}$ ($E_{1/2} = 0.54$ V, $\Delta E_{1/2} = 65$ mV, $i_a/i_c = 0.93$) the latter failing to show redox splitting. Therefore, the potentials for subsequent oxidations of the two trovacene units in $\mathbf{3}^{\bullet}$ differ

(8) The structure of the parent complex $\mathbf{1}^{\bullet}$ had been determined previously, although at low precision ($R = 0.186$ for 969 observed reflections): Engebretson, G.; Rundle, R. E. *J. Am. Chem. Soc.* **1963**, *85*, 481.

(9) (a) Etter, M. C. *Acc. Chem. Res.* **1990**, *23*, 120. (b) van Koningsveld, H. *Crst. Struct. Commun.* **1982**, *11*, 1423. (c) van Meurs, F.; van Koningsveld, H. *J. Organomet. Chem.* **1974**, *78*, 229.

Table 1. Crystallographic Data for Compounds **2•**, **2•**-d_1, and **3••**

compd	**2•**	**2•**-d_1	**3••**
crystal size (mm)	0.27 × 0.09 × 0.05	0.60 × 0.20 × 0.15	0.50 × 0.20 × 0.10
crystal system	monoclinic	monoclinic	monoclinic
space group	$P2_1/n$, $Z = 4$	$P2_1/n$, $Z = 4$	$P2_1/n$, $Z = 8$
lattice constants (pm/deg)	$a = 698.0(1)$, $\alpha = 90$	$a = 699.3(1)$, $\alpha = 90$	$a = 1353.4(1)$, $\alpha = 90$
	$b = 1654.1(1)$, $\beta = 104.60(1)$	$b = 1653.9(1)$, $\beta = 104.60(1)$	$b = 2327.6(1)$, $\beta = 104.34(1)$
	$c = 954.4(1)$, $\gamma = 90$	$c = 955.4(1)$, $\gamma = 90$	$c = 1358.2(1)$, $\gamma = 90$
vol. (nm^3)	1.0663(2)	1.0693(2)	4.1453(5)
formula sum	$C_{13}H_{12}O_2V$	$C_{13}H_{11}DO_2V$	$C_{26}H_{22}O_3V_2$
formula wt	251.17	252.17	968.63
density (calc.) (Mg/m^3)	1.565	1.566	1.552
absorpt-coeff (mm^{-1})	0.909	7.588	7.771
$F(000)$	516	516	1948
diffraktometer used	Enraf Nonius CAD4	Enraf Nonius CAD4	Enraf Nonius CAD4
wave length	MoKα (71.073 pm)	CuKα (154.178 pm)	CuKα (154.178 pm)
T (K)	213(2)	213(2)	213(2)
Θ range (deg)	2.46−26.30	5.35−64.93	3.80−54.96
index range (h,k,l)	−8/8,0/20,−11/0	−8/7,−19/0,0/11	−14/13,−24/0,0/14
scan type	Omega	Omega/2Theta	Omega/2Theta
program data collection	CAD4 EXPRESS	CAD4 EXPRESS	CAD4 EXPRESS
data reduction	XCAD4 (Harms, 1993)	XCAD4	XCAD4
no. of collected refl	2296	1927	5457
no. of unique refl	2168 [R(int) = 0.0480]	1817 [R(int) = 0.0791]	5199 [R(int) = 0.0489]
no. of obs. refl ($>2\sigma(I)$)	1393	1625	3948
no. of used refls	2168	1817	5199
absorpt correction	none	DIFABS	ψ-scans
max. and min. transmission			0.676, 0.353
structure solution	direct methods	direct methods	direct methods
structure refinement	full matrix on F^2	full matrix on F^2	full matrix on F^2
programs used	SHELXTL-PLUS (Siemens)	SHELXTL-PLUS	SHELXTL-PLUS
	SHELXL-96 (Sheldrick, 1996)	SHELXL-96	SHELXL-96
extinction coeff		0.0002(10)	0.00032(6)
weighting param $q1$ $q2$[a]	0.0507, 0	0.1708, 1.3499	0.0928, 1.3194
"goodness-of-fit" on F^2	1.022	1.152	1.013
e-max., min. [e/nm^3]	374, −335	586, −674	457, −412
no. of refined params	193	194	692
R (obsd refls)	0.0523	0.0666	0.0508
$wR2$ (used refls)	0.1155	0.2337	0.1430

[a] Weighting scheme: $w = 1/[\sigma^2(F_o^2) + (q1*P)^2 + q2*P]$ with $P = (F_o^2 + 2F_c^2)/3$.

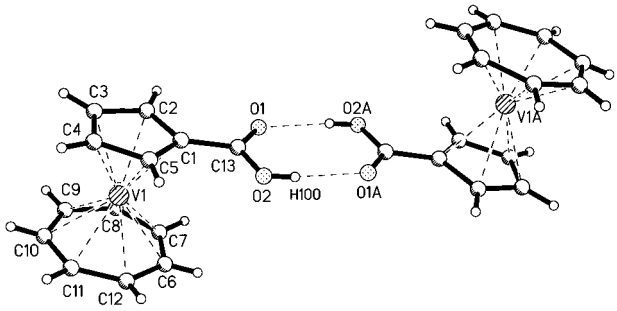

Figure 1. Molecular structure of (η^7-C_7H_7)V(η^5-C_5H_4COOH) (**2•**) with atom labeling scheme.

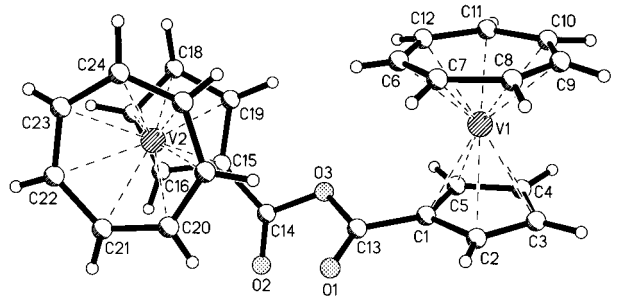

Figure 2. Molecular structure of [(η^7-C_7H_7)V(η^5-C_5H_4CO)]$_2$O (**3••**) with atom labeling scheme.

by less than ∼70 mV. As has been reported previously, secondary oxidation of trovacene manifests itself by an irreversible anodic wave at 1.03 V.[10] In the electrochemical medium, according to EPR spectroscopy, only the monomer **2•** is present.

The redox potential $E_{1/2}$(**2**$^{+/0}$) is pH dependent, a Nernst−Clark plot is depicted in Figure 3: metal centered oxidation is more facile by 144 mV for the carboxylate (η^7-C_7H_7)V(η^5-C_5H_4-COO^-) compared to the free acid **2•**. This cathodic shift falls short of the difference of 440 mV which we observed for the protonated and the neutral forms of (η^6-C_6H_6)Cr(η^6-C_5H_5N) where the influence on the redox behavior of the central metal, caused by the generation of a charge in the ligand sphere, is more direct.[11]

In polar and protic solvents **2•** is monomeric; **EPR spectroscopy** furnishes a coupling constant a(^{51}V) which is slightly pH dependent; the curve describing this function resembles the Nernst−Clark plot (Figure 3). In meticulously dried toluene the equilibrium 2 **2•** ⇌ (**2•**)$_2$, caused by hydrogen bonding, is set up as demonstrated by the superposition of the EPR spectra of the monoradical **2•** and the biradical (**2•**)$_2$[12] (Figure 4). Subtraction of the monomer spectrum which is accessible at higher temperature from the sum spectrum and simulation of the residual dimer spectrum yields the exchange coupling constant $J = -0.011$ cm^{-1}, this parameter being defined by the term $JS_1 \cdot S_2$ in the Hamiltonian.

The observation of a superposition of individual EPR spectra of the monomeric acid **2•** and its dimer (**2•**)$_2$ suggests that the lifetime of the components of the association equilibrium 2(**2•**)

(10) Elschenbroich, Ch.; Bilger; E.; Metz, B. *Organometallics* **1991**, *10*, 2823.

(11) Elschenbroich, Ch.; Koch, J.; Kroker, J.; Wünsch, M.; Massa, W.; Baum, G.; Stork, G. *Chem. Ber.* **1988**, *121*, 1983.

(12) A similar behavior has been reported for the radical 2,2,5,5-tetramethyl-Δ^3-pyrroline-3-carboxylic acid 1-oxyl: Veloso, D. P.; Rassat, A. *J. Chem. Res. (S)* **1979**, 168. J. *Chem. Res. (M)* **1979**, 1942.

Table 2. Selected Bond Distances (Å) and Angles (deg) in **2**• and **2**•-d_1

	2•	**2**•-d_1
Bond Distance (Å)		
V(1)−C(6)	2.177(5)	2.170(6)
V(1)−C(7)	2.179(5)	2.188(6)
V(1)−C(8)	2.173(4)	2.184(6)
V(1)−C(9)	2.172(4)	2.196(6)
V(1)−C(10)	2.183(4)	2.195(6)
V(1)−C(11)	2.177(5)	2.177(5)
V(1)−C(12)	2.181(5)	2.188(7)
V(1)−centroid C_7-ring	1.459(1)	1.465(3)
V(1)−C(1)	2.242(4)	2.253(5)
V(1)−C(2)	2.257(4)	2.267(6)
V(1)−C(3)	2.261(4)	2.257(6)
V(1)−C(4)	2.257(4)	2.272(6)
V(1)−C(5)	2.264(4)	2.256(5)
V(1)−centroid C_5-ring	1.9104(7)	1.9138(8)
C(6)−C(7)	1.396(7)	1.393(9)
C(7)−C(8)	1.415(7)	1.404(9)
C(8)−C(9)	1.417(7)	1.395(10)
C(9)−C(10)	1.401(7)	1.416(10)
C(10)−C(11)	1.390(7)	1.417(10)
C(11)−C(12)	1.406(7)	1.403(10)
C(12)−C(6)	1.393(7)	1.426(10)
weighted av C_7-ring bond distance	1.4018(27)	1.4074(37)
C(1)−C(2)	1.416(5)	1.424(8)
C(2)−C(3)	1.398(6)	1.408(8)
C(3)−C(4)	1.411(6)	1.404(9)
C(4)−C(5)	1.412(6)	1.415(8)
C(5)−C(1)	1.415(5)	1.425(7)
weighted av C_5-ring bond distance	1.4100(28)	1.4164(34)
C(1)−C(13)	1.459(5)	1.466(7)
C(13)−O(1)	1.235(4)	1.235(6)
C(13)−O(2)	1.305(5)	1.309(6)
O(2)−H/D(100)	0.79(5)	0.84(9)
H/D(100)−O(1A)	1.86(5)	1.80(9)
O(2)−O(1A)	2.637(4)	2.642(5)
V(1)−V(2)	10.1046(17)	
Bond Angles (deg)		
C(6)−C(7)−C(8)	128.6(5)	128.4(6)
C(5)−C(1)−C(2)	108.1(4)	108.2(5)
C(5)−C(1)−C(13)	126.6(4)	125.0(5)
O(1)−C(13)−O(2)	123.8(4)	124.0(5)
C(13)−O(2)−H/D(100)	108(3)	112(6)
O(2)−H/D(100)−O(1A)	168(5)	176(9)
Torsion Angles (deg)		
C(2)−C(1)−C(13)−O(1)	−0.3(6)	−1.0(8)
weighted av tor angles at C_5-ring	0.88(23)	1.00(28)
weighted av tor angles at C_7-ring	1.10(34)	1.51(45)

$\rightleftharpoons$ (**2**•)$_2$ exceeds the EPR time scale. This conforms with the kinetics of self-association of benzoic acid which have been studied extensively in the past.[13] From ultrasonic absorption measurements the rate constant $k_d = 3.3 \times 10^6$ at 20° has been derived for the dissociation of benzoic acid dimers in benzene. Thus, the lifetime of individual carboxylic acid dimers is long on the EPR hyperfine time scale, defined by $a(^{51}\text{V}, \mathbf{2}^{\bullet}) = -7.34$ mT $\cong 2.05 \times 10^8$ s^{-1}, and the species **2**• and (**2**•)$_2$ should be detectable simultaneously. The equilibrium constant $K_{20°} = 2.4 \times 10^3$ for the process 2 (**2**•) $\rightleftharpoons$ (**2**•)$_2$ can be inferred from the monomer/dimer ratio which governs the superposition spectrum. Not surprisingly, this constant is very similar to the respective value for the self-association of benzoic acid, $K_{20°} = 8.9 \times 10^3$,[13] in the same solvent. From the temperature dependence of the equilibrium composition (Figure 5) the value $\Delta H = -11.8$ kcal/mol per pair of hydrogen bonds is obtained. An analogous procedure carried out for the deuterated acid (η^7-C_7H_7)V(η^5-C_5H_4COOD), **2**•-d_1, led to $\Delta H = -15.2$ kcal/mol. These data agree with those determined by means of IR spectroscopy for the association of benzoic acid (PhCOOH: −10.6, PhCOOD: −15.8 kcal/mol),[14] and concord with the conclusion reached from recent SCF and correlated MP2 calculations, that in complexes pairing neutral molecules, deuterium bonds appear to be stronger than hydrogen bonds.[15] Replacing the hydrogen bond in **2**• by a deuterium bond may, in principle, have two

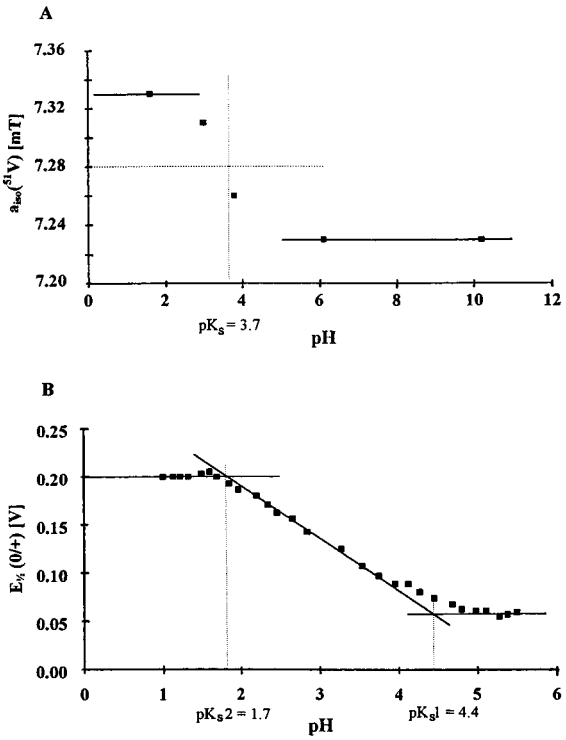

Figure 3. Plots of the redox potential $E_{1/2}$ ($\mathbf{2}^{+/0}$) and of the coupling constant $a(^{51}\text{V}, \mathbf{2}^{\bullet})$ vs pH.

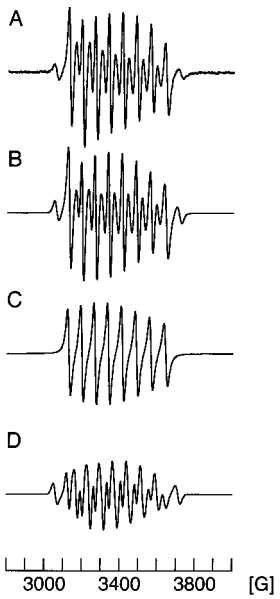

Figure 4. (A) EPR spectrum (9.4076 GHz) of the trovacenylcarboxylic acid (**2**•) in toluene at 295 K, $\langle g \rangle = 1.9809$, $a(^{51}\text{V}) = -7.34$ mT. (B) Simulated trace, generated by superposition of the spectra of the monomer **2**• and the dimer (**2**•)$_2$ in the ratio 2:3. (C) Simulated spectrum of the monomer **2**•, $\langle g \rangle = 1.9809$, $a(^{51}\text{V}) = -7.34$ mT. (D) Simulated spectrum of the dimer (**2**•)$_2$, $\langle g \rangle = 1.9810$, $a(^{51}\text{V}) = -7.42$ mT, $J = -0.011$ cm^{-1}.

(13) (a) Maier, W. *J. Chim. Phys.* **1964**, *61*, 239. (b) Borucki, L. *Ber. Bunsenges. Phys. Chem.* **1967**, *71*, 504. (c) Rassing, J.; Østerberg, O.; Bak, T. A. *Acta Chem. Scand.* **1967**, *21*, 1443.

(14) Glasoe, P. K.; Hallock, S.; Hove, M.; Duke, J. M. *Spectrochim. Acta* **1971**, *27A*, 2309.

(15) Scheiner, S.; Cuma, M. *J. Am. Chem. Soc.* **1996**, *118*, 1511.

Table 3. Selected Bond Distances (Å) and Angles (deg) in **3•••**

	3•••		
	Bond Distances (Å)		
V(1)−C(6)	2.173(6)	V(1)−C(1)	2.250(5)
V(1)−C(7)	2.183(6)	V(1)−C(2)	2.280(5)
V(1)−C(8)	2.181(7)	V(1)−C(3)	2.280(6)
V(1)−C(9)	2.183(6)	V(1)−C(4)	2.263(6)
V(1)−C(10)	2.179(6)	V(1)−C(5)	2.235(6)
V(1)−C(11)	2.166(6)	V(1)−centroid C_7-ring	1.461(8)
V(1)−C(12)	2.163(6)	V(1)−centroid C_5-ring	1.918(8)
C(6)−C(7)	1.406(10)	C(1)−C(2)	1.422(8)
C(7)−C(8)	1.408(10)	C(2)−C(3)	1.384(8)
C(8)−C(9)	1.379(10)	C(3)−C(4)	1.411(8)
C(9)−C(10)	1.386(9)	C(4)−C(5)	1.395(8)
C(10)−C(11)	1.399(10)	C(5)−C(1)	1.421(8)
C(11)−C(12)	1.400(10)	av C_7-ring bond distance	1.3968(43)
C(12)−C(6)	1.399(12)	av C_5-ring bond distance	1.4068(34)
C(1)−C(13)	1.459(7)	O(3)−C(14)	1.414(6)
C(13)−O(1)	1.197(6)	C(14)−O(2)	1.195(7)
C(13)−O(3)	1.376(6)	V(1)−V(2)	6.664(1)
	Bond Angles (deg)		
C(1)−C(2)−C(3)	107.3(5)	C(6)−C(7)−C(8)	128.5(6)
C(13)−C(1)−C(2)	124.8(5)	O(3)−C(13)−O(1)	122.5(5)
	Torsion Angles (deg)		
weighted av tor angles at C_5-ring	0.60(28)	C(1)−C(13)−C(2)−C(3)	174.5(5)
weighted av tor angles at C_7-ring	1.79(44)	C(14)−O(3)−C(13)−O(1)	25.0(8)

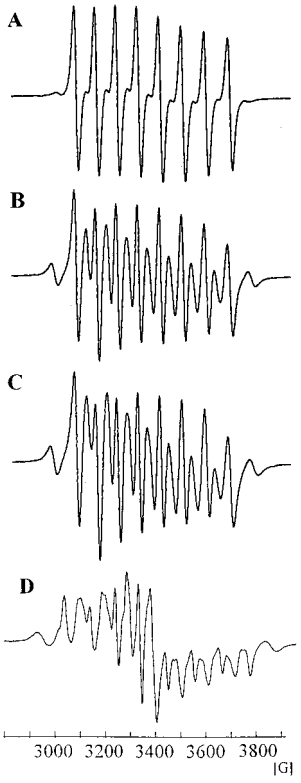

Figure 5. Temperature dependence of the equilibrium 2(**2•**) ⇌ (**2•**)$_2$ as demonstrated by EPR, solvent: toluene: (A) 335 K (9.3999 GHz), (B) 280 K (9.4025 GHz), (C) 260 K (9.4022 GHz), (D) 96 K (9.4126 GHz).

effects on the EPR spectrum, namely a shift in the equilibrium position caused by the differing strengths of these two bonds and a modification of the extent of exchange coupling due to the change of the chemical nature of the spacer. Whereas the former effect clearly manifests itself in different ratios of monomer to dimer for **2•** and **2•**-d_1 whose temperature dependence yielded the values for the bond enthalpies stated above, the aggregate spectra of the monomer/dimer mixtures of **2•** and **2•**-d_1, respectively, exhibited insufficient detail to deduce with

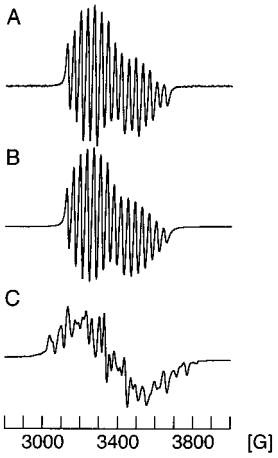

Figure 6. EPR spectrum of trovacenylcarboxylic acid anhydride **3•••** in toluene. (A) 295 K (9.0937 GHz). (B) Simulated trace, $\langle g \rangle = 1.9819$, $a(^{51}\mathrm{V}) = -7.32$ mT, $J = -0.345$ cm^{-1}. (C) 90 K (9.4195 GHz).

confidence that an isotope effect on exchange coupling J is operative.

The covalently linked counterpart **3•••** also yields a typical biradical EPR spectrum (Figure 6) from which the exchange coupling constant $J = -0.345$ cm^{-1} can be derived. While an evaluation of the J values for (**2•**)$_2$ and **3•••** based on metal−metal distances is unwarranted because both species are flexible in fluid solution, the number of intervening bonds, eight for (**2•**)$_2$ and six for **3•••**, may be a more reliable criterion. We have studied exchange coupling in organometallic biradicals with 3−8 bonds separating the two spin-bearing V(d^5) central metals[16] and find the J values to follow a steady trend if plotted against the number of intervening bonds although the chemical nature of the bridges differs profoundly. A similar bond-counting strategy has been proposed to assess the gradation of the rates

(16) (a) Elschenbroich, Ch.; Heck, J. *Angew. Chem., Int. Ed. Engl.* **1981**, *20*, 267. (b) Elschenbroich, Ch.; Bretschneider-Hurley, A.; Hurley, J.; Massa, W.; Wocadlo, S.; Pebler, J.; Reijerse, E. *Inorg. Chem.* **1993**, *32*, 5421. (c) Elschenbroich, Ch.; Bretschneider-Hurley, A.; Hurley, J.; Behrendt, A.; Massa, W.; Wocadlo, S.; Reijerse, E. *Inorg. Chem.* **1995**, *34*, 743. (d) Elschenbroich, Ch.; Metz, B.; Neumüller, B.; Reijerse, E. *Organometallics* **1994**, *13*, 5072.

of long-distance electron-transfer along protein pathways, the view being taken that the decay per bond is not very sensitive to the different bond types in the chain.[1c] Even the hydrogen bond in its mediation property appears to be approximately equivalent to two covalent bonds.[17] This is supported by the observations that ET through hydrogen-bonded interfaces is fast[4i] and that in a number of hydrated metal salts hydrogen bonds between nearest neighbor transition metal ions constitute magnetic exchange propagating pathways.[18]

Before an attempt is made to advance a conceivable mechanism for the exchange coupling in the dimer $(\mathbf{2}^{\bullet})_2$, the question must be addressed whether an "open" dimer may be present, in which the eight-membered ring $-$COOHHOOC$-$ has been cleaved and a single hydrogen bond forms the connecting link between two trovacene units. This type of scission has been proposed for the acetic acid dimer in acetone solution[19a] and for a number of derivatives of acetic acid as well.[19b] For the following reasons we exclude this possibility in the case of trovacenyl carboxylic acid ($\mathbf{2}^{\bullet}$): (1) If a saturated solution of $\mathbf{2}^{\bullet}$ in toluene (3.3×10^{-3} mol l^{-1}) is diluted, EPR reveals that the equilibrium 2 ($\mathbf{2}^{\bullet}$) $\rightleftharpoons$ $(\mathbf{2}^{\bullet})_2$ is shifted to the left to an extent governed by the value of K. (2) The enthalpy changes $\Delta H =$ 11.8 kcal mol^{-1} [$(\mathbf{2}^{\bullet})_2$] and 15.2 kcal mol^{-1} [$(\mathbf{2}^{\bullet}$-$d_1)_2$] are too large for the cleavage of one hydrogen bond only. (3) The entropy change $\Delta S = 32$ cal deg^{-1} mol^{-1} clearly points to an enhancement of the number of particles.

In the realm of exchange coupled systems, the fundamental question, of course, deals with the alternatives of direct ("through space", orbital overlap) or indirect ("through bond", superexchange) propagation. The large intervanadium distance of 10.10 Å (trans) respectively 9.10 Å (cis) in the metal centered biradical $(\mathbf{2}^{\bullet})_2$ renders the direct variant improbable and suggests a closer inspection of the nature of the connecting link. Since we have determined the exchange coupling constant J from EPR spectra recorded in fluid solution, bond angles which are of pivotal importance for the sign and magnitude of J [20] are not fixed. At this stage, we therefore only qualitatively delineate a pathway for exchange coupling which explicitly takes into account the hydrogen bridge as a part of the link connecting the two paramagnetic V(d^5) centers. Exchange interaction can be regarded as a borderline case of a very weak chemical bond. Therefore, the presence of small spin densities on the hydrogen and oxygen atoms of the hydrogen bond may be responsible for the electron−electron spin−spin coupling observed for $(\mathbf{2}^{\bullet})_2$. In order to assess the spin density on the carboxylic proton we have recorded the ^{1}H NMR spectrum of the monomeric acid $\mathbf{2}^{\bullet}$ (Figure 7). In addition to very broad signals at δ 315 (H6−H12), δ 146.2 (H2,5) and δ 127.6 (H3,4) a resonance at δ 14.15 is observed which, relative to the diamagnetic organometallic acid Cr(η^6-$C_6H_5COOH)_2$, is shifted to lower field by 3 ppm. According to the relation $\Delta H/H = -a(^1H)g_{av}\ \beta S(S+1)(g_H\beta_H 3kT)^{-1}$ this contact shift can be converted into the isotropic hyperfine coupling constant $a(^1H_{COOH}, \mathbf{2}^{\bullet}) = 0.0042$ mT.[21] While it would be difficult to quantitatively relate this value to the observed exchange coupling constant J of the dimer $(\mathbf{2}^{\bullet})_2$, the proof of finite spin density on the H atom of the hydrogen bridge nevertheless constitutes evidence that a through bond mechanism may contribute to the communication between the two paramagnetic centers in $(\mathbf{2}^{\bullet})_2$. The role, correlated proton motion within the hydrogen bonds,[22] plays in the generation of exchange coupling would be another interesting aspect to explore.

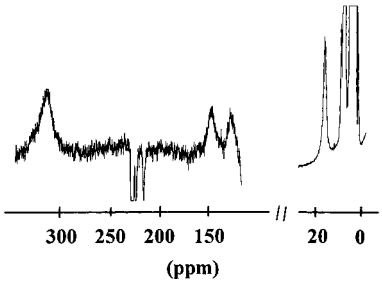

Figure 7. ^{1}H NMR spectrum (500 MHz) of trovacenylcarboxylic acid ($\mathbf{2}^{\bullet}$) in THF-d_8 at 295 K.

In a more general context, the trovacenyl unit (η^7-C_7H_7)V-(η^5-C_5H_4-) promises to become a versatile paramagnetic probe rivaling the organic nitroxides. This derives from its fairly robust nature,[10] ease of derivatization via regioselective lithiation at the Cp ring,[23] and the favorable EPR properties which should permit detailed study of intermetallic communication in the range 100 $a(^{51}V) > J > 0.01\ a(^{51}V)$ wherein $a(^{51}V, \mathbf{1}^{\bullet}) = 66 \times 10^{-4}$ cm^{-1}. Furthermore, applications of the trovacenyl group in bioorganometallic chemistry[24] and in the construction of paramagnetic metallomesogens[25] are conceivable.[26] Here the study of orientational phenomena should profit from the high anisotropy of the ^{51}V hyperfine interaction in $\mathbf{1}^{\bullet}$ ($A_{\parallel} = -1.39$ mT, $A_{\perp} = -9.61$ mT).

Acknowledgment. This work was supported by the Volkswagen Foundation and the Fonds der Chemischen Industrie. We are indebted to Professor P. H. Rieger for his help in introducing m_I-dependent line width effects into the simulation program. This article is dedicated to Professor Walter Siebert on the occasion of his 60th birthday.

Supporting Information Available: X-ray crystallographic data for $\mathbf{2}^{\bullet}$, $\mathbf{2}^{\bullet}$-d_1, and $\mathbf{3}^{\bullet\bullet}$ including tables of atomic coordinates, bond angles and bond lengths (20 pages). See any current masthead page for ordering and Internet access instructions.

JA964445S

(17) de Rege, P. J. F.; Williams, S. A.; Therien, M. J. *Science* **1995**, *269*, 1409.

(18) (a) Hendrickson, D. N. In *Magneto-Structural Correlations in Exchange Coupled Systems*; Willet, R. D., Gatteschi, D., Kahn, O., Eds.; *NATO ASI Series*; Reidel: Dordrecht, 1985; pp 523−554. (b) Bossek, U.; Wieghardt, K.; Nuber, B.; Weiss, J. *Angew. Chem., Int. Ed. Engl.* **1990**, *29*, 1055. (c) Goodson, P. A.; Glerup, J.; Hodgson, D. J.; Michelsen, K.; Rychlewska, U. *Inorg. Chem.* **1994**, *33*, 359. (d) Arulsamy, N.; Glerup, J.; Hodgson, D. J. *Inorg. Chem.* **1994**, *33*, 2066. (e) Moreno, J. M.; Ruiz, J.; Dominguez-Vera, J. M.; Colacio, E. *Inorg. Chim. Acta* **1993**, *208*, 111. Muhonen, H. *Inorg. Chem.* **1986**, *25*, 4692. Bertrand, J. A.; Fujita, E.; Van Derveer, D. G. *Inorg. Chem.* **1980**, *19*, 2022.

(19) (a) Corsaro, R. D.; Atkinson, G. *J. Chem. Phys.* **1970**, *54*, 4090. (b) Sano, T.; Tatsumoto, N.; Niwa, T.; Yasunaga, T. *Bull. Chem. Soc. Jpn.* **1972**, *45*, 2669. Sano, T.; Tatsumoto, N.; Mende, Y.; Yasunaga, T. *Bull. Chem. Soc. Jpn.* **1972**, *45*, 2673.

(20) Bencini, A.; Gatteschi, D. *EPR of Exchange Coupled Systems*; Springer-Verlag: Berlin, 1990; Chapter 1. Kahn, O. *Molecular Magnetism*; VCH Publishers: New York, 1993; Chapter 8.

(21) Due to the nearly isotropic g tensor ($g_{\parallel} - g_{\perp} = 0.02$), the large distance from and the geometrical disposition of the carboxylic proton to the central metal atom in $\mathbf{2}^{\bullet}$, a pseudocontact contribution can be neglected. See: Elschenbroich, Ch.; Gerson, F. *J. Organomet. Chem.* **1973**, *49*, 445.

(22) Horsewill, A. J.; McDonald, P. J.; Vijayaraghavan, D. *J. Chem. Phys.* **1994**, *100*, 1889. Stöckli, A.; Meier, B. H.; Kreis, R.; Meyer, R.; Ernst, R. R. *J. Chem. Phys.* **1990**, *93*, 1502.

(23) Groenenboom, C. J.; de Liefde Meijer, H. J.; Jellinek, F. *Recl. Trav. Chim. Pays. Bas.* **1974**, *93*, 6.

(24) Jaouen, G.; Vessières, A.; Butler, I. S. *Acc. Chem. Res.* **1993**, *26*, 361.

(25) Alonso, P. J. In *Metallomesogens. Synthesis, Properties, and Applications*; Serrano, J. L., Ed.; VCH: Weinheim, 1996.

(26) As an example, we have prepared trovacenylcholesterol and are currently exploring its physical properties: Schiemann, O., Elschenbroich, Ch. Unpublished.